High Efficiency GPS Block-III RF Front-End Supporting Multi-Code and Multi-Carrier Waveforms

Toshifumi Nakatani, J. Johana Yan, Houman Ghajari
MaXentric Technologies, LLC
La Jolla, CA 92037
Email: tnakatani@maxentric.com

Aly E. Fathy
Department of EE & CS
University of Tennessee Knoxville
Knoxville, TN 37996
Email: afathy@utk.edu

Donald F. Kimball
pSemi Corporation
San Diego, CA 92121
Email: dkimball@ieee.org

***Abstract*—A high power and high efficiency RF transmitter front-end is developed for a GPS block-III satellite payload. The transmitter consists of two 400-W_{peak} power amplifiers (PAs) and diplexer. The PAs amplifies L1 signal at 1575 MHz and L2 and L5 composite signal at 1200 MHz respectively. The delivered power is combined by the diplexer. This topology promises significantly reduced size, weight, and power dissipation provided the higher peak to average power ratio and linearity challenges can be addressed. In response to these challenges, envelope tacking technology is adopted to reduce the overall DC power consumption, size, and weight of the rad-hard SSPA for the GPS Block-III L-band. We demonstrate an RF front-end sub-system prototype, which successfully delivers all L1, L2 and L5 signals with total 370-W_{avg} output power.**

Keywords— High power amplifiers, multiplexer, GaN FET, envelope tracking, efficiency, Global Positioning System.

I. INTRODUCTION

The Global Positioning System (GPS) modernization program is an ongoing, multibillion-dollar effort to upgrade the GPS space and control segments with new features to improve Position, Navigation and Timing (PNT) performance [1]. There are several challenges for the RF front-end to support new functions while maintaining minimal size, weight and power.

The legacy GPS satellites service two frequency channels (i.e. L1: 1575.42 MHz and L2: 1227.6 MHz), separated by 350 MHz. For modernized GPS, the additional L5 (1176.42 MHz), located only at 51 MHz apart from the L2, is provided. It is desired to have the minimal number of antennas on the satellite. Combining the all GPS signals enable the number of antennas to be reduced. However, it is challenging to combine the outputs of the three bands to one antenna with sufficient isolation due to the narrow channel separation between L2 and L5, resulting in trade-off between increased size and weight versus insertion losses of a triplexer.

The proposed solution is to use a diplexer by combing the L2 and L5 bands together (denoted L2/L5), to reduce the hardware, while mitigating the isolative challenge to the software domain and leveraging the recent advance in digital technologies, as described later. Two transmitters and a comb-line diplexer are placed together as a system level solution for GPS Block-III. The L2 and L5 signals are upconverted in a dual band fashion. A comb-line diplexer is much easier to design and combines these inputs with very low insertion losses in a compact form factor.

The next challenge is amplification of the signals. The legacy GPS waveform consists of two BPSK codes, C/A and P(Y), where the envelope of the RF waveform is ideally constant. Three more codes, M, L1C pilot and data, are to be serviced at the L1 band (1575.42 MHz) in the modernized GPS. The envelope of the linearly combined waveform with more than two codes is non-constant, which leads to PA efficiency degradation in conventional power amplifiers (PAs). The alternative is to force a constant envelope waveform through the PA by adding power in the code. Since the power is not necessary, this results in code inefficiency, which nevertheless is still power wasted.

We hereby proposed a novel PA architecture that addresses this degradation and maintains high efficiency in the presence of such waveforms. The architecture is applied to amplification of the L2/L5 composite signal, which also has non-constant envelope.

Recently, GaN solid-state PAs (SSPAs) with peak output power of >300 W have been reported for L-band satellite applications [2, 3]. A GaN SSPA is promising replacement to the traveling wave tube amplifier (TWTA) in terms of high efficiency and reliability (radiation hardening, etc.). The reported GaN SSPAs achieved high efficiency at the peak power under cosine-wave (CW) test. However, as we just mentioned, the efficiency decreases when the modulated signals supporting multi-code and multi-carrier waveforms are delivered due to back-off operation.

In response to the challenges of amplification, envelope tacking (ET) technology [4] is adopted to reduce the overall DC power consumption, size, and weight of the rad-hard SSPA [5] for the GPS Block-III L-band as shown in Fig. 1. Under envelope tracking, the supply voltage of the SSPA is dynamically adjusted by the envelope amplifier (EA) to follow the envelope of the RF signal. As a result, the RF amplifier is kept near saturation throughout the dynamic variations of the signal, improving the average efficiency. This technique can simultaneously support normal and boost mode, multi-carrier, and multi-code waveforms well beyond the 5-code L1 band.

The third challenge is signal fidelity. In this work, a two-step digital predistortion (DPD) procedure is employed, which consists of 1) memoryless polynomial-based predistortion, 2) point-to-point residue error correction. The proposed DPD linearizes the group delay variation over instantaneous amplitude modulation and suppresses the intermodulation of the L2/L5 composite signal.

II. Proposed GPS-III RF Front-End Sub-System

A. Overall Architecutre

Fig. 1 shows the block diagram of the proposed GPS Block-III RF front-end sub-system. It is desired to have the minimal number of antennas on the satellite. Combining the all GPS signals enables the number of antennas to be reduced. The additional L5 band (1176.45 MHz) is an issue because it is spectrally close to the L2 band (1227.6 MHz), where the straightforward brute force method of using a triplexer results in increased size and weight or insertion losses. The solution is to use a diplexer by combing the L2 and L5 bands together (denoted L2/L5).

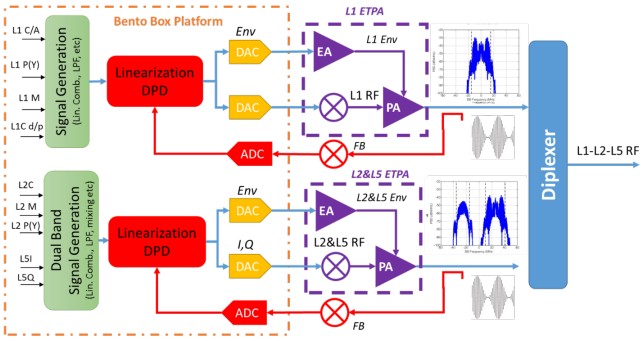

Fig. 1. Block diagram of GPS Block-III RF front-end sub-system.

The L1 and L2/L5 PAs operate under ET to enhance the efficiency. In the digital baseband, the 5 codes for L1 are linearly combined and pre-distorted for linearizing the L1 ETPA. Both the 3 codes for L2 and the 2 codes for L5 are combined of a dual carrier signal and pre-distorted for linearizing the L2/L5 ETPA. Envelope modulated voltages of both L1 and L2/L5 are separately generated. These functions are implemented into MaXentric's BentoBox platform [6].

B. Diplexer

Fig. 2 shows the (a) photo and (b) internal CAD drawing of the hollow resonators of the fabricated high-power diplexer.

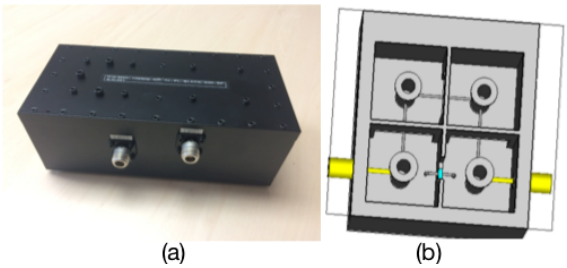

Fig. 2. (a) Photo and (b) hollow resonators of fabricated comb-line diplexer.

The simulated characteristics of the triplexer (conventional) and the diplexer (proposed) are summarized in Table I. The simulated insertion losses of the diplexer are 0.1-0.3 dB at L1, L2 and L5 frequencies while those of the triplexer are 0.3-0.8 dB. The measured insertion losses of the diplexer are 0.2-0.4 dB. The size and weight of the diplexer is 2000 cm^3 and 3.5 kg respectively. Using the hollow resonator structure, the simulated power tolerance of the multipactor process is 400-1890 W.

TABLE I. Simulated Characteristics of Multiplexers.

	Triplexer			Diplexer (Proposed)		
Band	L1	L2	L5	L1	L2	L5
Loss (dB)	0.26	0.58	0.76	0.31	0.22	0.13
Size (cm^3)		3000			2000	
Weight (kg)		5.3			3.5	
Multipaction (W)	—	—	—	1887	459	556

III. L1-Band GaN SSPA Under ET Operation

A. Overview of ET-PA Module

Fig. 3 shows the block diagram of the ET-PA, comprising bottom and top boards. One of challenges for an ET-PA with more than 2-way combining is stability. If the layout of the unit blocks consisting of RF amplifier and EA is asymmetry, current distribution will not be uniformed. The current captured either continuously increases or periodically increases and decreases due to temperature imbalance. To maintain the symmetry, the 3D structure is employed, where 2-stage driver stage and 4-way final stage are accommodated in the bottom board and the four identical EAs are in the top board. To realize 150-MHz envelope modulation bandwidth, each EA supplies a modulated voltage to each RF amplifier through a short connector (22.5 mm). Another merit of the 3D structure is that heat generated in the RF amplifier and EA are sunk from bottom and top sides separately, which ideally provides half thermal resistance, compared to a single board implementation.

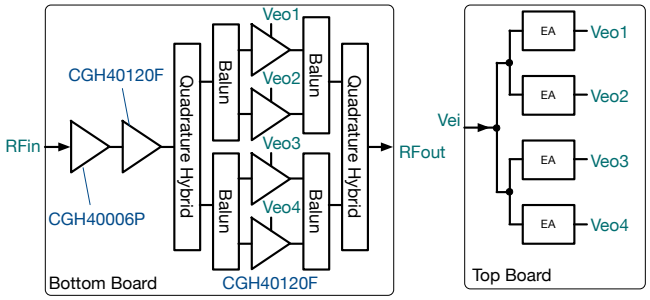

Fig. 3. Block diagram of 460-W_{peak} / 230-W_{avg} ET-PA module.

B. Balanced / Push-Pull RF Amplifier Design

Fig. 4 shows (a) the output-side PCB layout and (b) the EM-simulated load impedance seen from an GaN FET device used for the final-stage RF amplifier. Wolfspeed 120-W FETs (CGH40120F) are used. JPL tested the radiation tolerance and no significant degradation was observed [4]. The board material is Rogers low outgassing woven glass reinforced laminate (AD1000). The load impedance is optimized to achieve highest CW efficiency at the supply voltage of 23 V, which is the RMS value of the envelope waveform. Initially, using a quarter wave-length line at the carrier frequency (f_0) as the drain bias line, the load impedance at $2f_0$ becomes almost short, and the load impedance at $3f_0$ is tuned to be relatively high (i.e. close to Class-F operation). After that, the impedance is experimentally optimized to achieve high efficiency.

Fig. 5 (a) shows the PCB layout of the output power combiner. To compromise between small size and low insertion

loss, the characteristic impedance (Z_0) is set to 25 Ω. To avoid using edge coupling between transmission lines and achieve high breakdown power in vacuum environment (multipaction [7]), on-board rat-race baluns and branch-line quadrature hybrid coupler (QHC) are employed. A ring-type rat-race balun reduces the radiation loss. After the QHC, 35.4-Ω $\lambda/4$ transmission line converts Z_0 to 50 Ω.

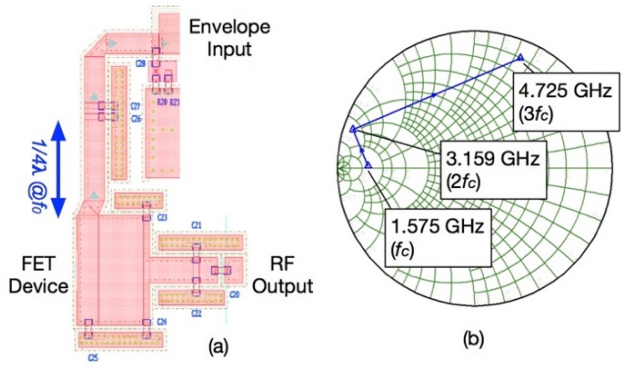

Fig. 4. (a) PCB layout of output matching network and (b) EM-simulated load impedance seen from FET device (initial design, Z_0 = 25 Ω).

Figs. 5 (b, c) show the simulated total insertion loss and return loss of each RF input over frequency. At the L1 band, the insertion loss of 0.23 dB and the return losses of <-25 dB are achieved using the AWR AXIEM.

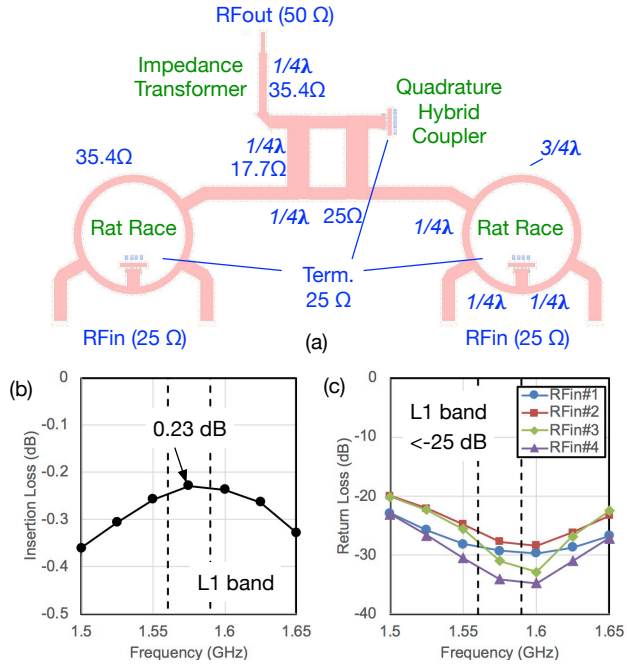

Fig. 5. (a) PCB layout of output power combiner and (b, c) simulated total insertion loss and return loss of each RF input over frequency.

C. Single Envelope Amplifier (EA) Circuit

Fig. 6 shows the schematic of a 150-MHz EA, consisting of switching and linear stages. A transformer coupled feedback current sensor, merged with a faster direct coupled gate drive level shifter, gives the design advantages over the conventional EA, which required careful adjustment to maximize efficiency while in use. Floating gate driver is employed to drive an N-type FET of an asynchronous switcher for high efficiency. The current sensor output is provided to the floating circuits through hysteresis comparator and digital isolator.

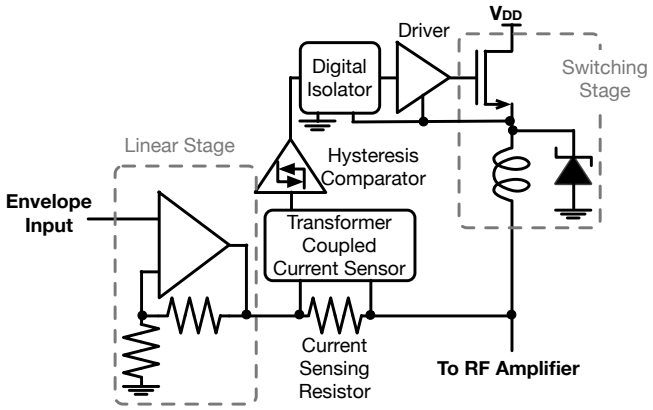

Fig. 6. Schematic of wideband high efficiency EA.

Fig. 7 shows the measured and original (a) waveform and (b) power spectral density of the EA. The results were obtained from 1 of 4 cylinders with a 5.9-Ω high power resistor. The measured output power, efficiency and absolute RMS error were 85 W_{avg}, 78% and 4.2% respectively. The measured voltage waveform follows the original voltage waveform. The developed EA covers 150 MHz frequency range although a small peaking is observed in the low power region (~50 MHz).

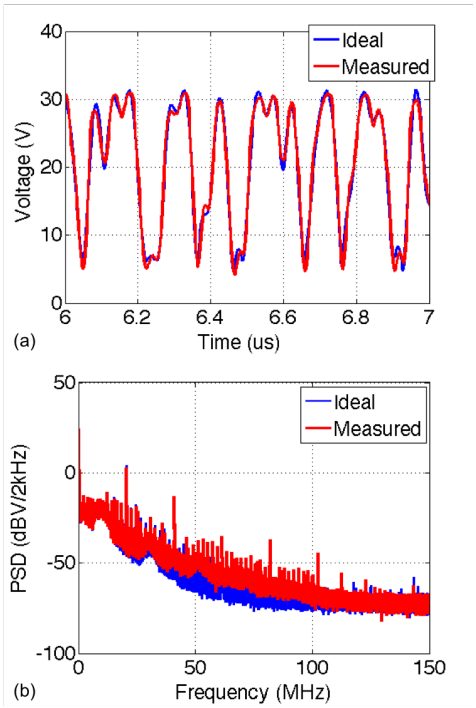

Fig. 7. Measured and ideal (a) waveforms and (b) power sepctral densities delivered from EA.

D. Fabricated ET-PA Module

Fig. 8 shows the (a) case structure and (b) photo of the ET-SSPA module. The size of the Aluminium case is 292 mm x 244 mm x 51 mm. To prevent EMI from EA to RF amplifier, a shield is inserted between them. The EA and RF amplifier are connected through the four-small holes of the shield. Excellent thermal management is realized by separating the heat generated at the EA and RF amplifier and individually channeling it from the top and bottom plates, respectively. For initial test purpose, finned heatsinks are used but they will be replaced with heat pipes for vacuum environment.

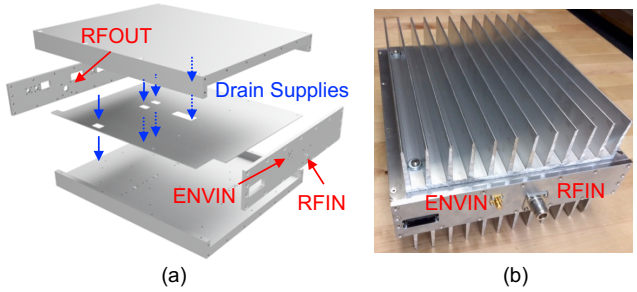

Fig. 8. (a) Case structure and (b) photo of fabricated ET-SSPA module.

IV. Two-Step Digital Predistortion

In this work, a two-step DPD procedure is employed: 1) memoryless polynomial-based predistortion, 2) point-to-point residue error correction. In the 1st step, a distorted waveform, *yI*, is captured and a pre-distorted waveform, *xpI*, is calculated. In the 2nd step, another distorted waveform, *ypI*, is captured and a pre-distorted waveform, *xrI*, is calculated from

$$xrI = xpI - (ypI - xI) \quad (1)$$

where the average peaks of *xpI*, *ypI* and *xI* are identical. The 2nd step is applied iteratively by replacing *xpI* with previous *xrI*. The whole process is repeated until the output of the PA is linearized. Generic approaches, such as memory polynomial DPD [8], are applicable alternative to point-to-point correction for future implementation.

V. Experimental Results

A. Diplexer

The measured insertion losses of the diplexer are summarized in Table II. They are between 0.2 dB and 0.35 dB as expected.

TABLE II. Measured Insertion Loss of Diplexer.

	L1	L2	L5
Insertion Loss	0.35 dB	0.24 dB	0.23 dB

B. L1-Band GaN SSPA under ET Operation

When an imitated L1-band signal with the peak-to-average ratio of 3 dB is applied, the gain is 43 dB as expected from the CW test. The DE and PAE are 50% and 45% respectively at the peak / average output power of 464 W_{peak} / 232 W_{avg}. Based on the CW measurement, the DE of the RF amplifier is 64% and the corresponding efficiency of the EA is 78%. The efficiency here accounts for the overall transmitter sub-system, including the code efficiency (99%).

Using the proposed DPD, the measured normalized RMS error (NRMSE) decreases to 3.5% from 7.8%. The corresponding overall correlation loss is 0.01 dB (see Appendix), which is very small compared with the requirements of a GPS receiver (C/A: 0.3 dB, P(Y): 0.6 dB, L1C: 0.2 dB [9], [10]). The performance before and after adaptive DPD is summarized in Table III.

TABLE III. Measured Performance Before and After DPD.

DPD	P_{avg}	Gain	DE	PAE	C.L.
No	229 W	42.7 dB	49.9%	45.1%	0.05 dB
Memory	232 W	42.6 dB	50.1%	45.2%	0.01 dB

Fig. 9 shows the measured (a) AM-AM and (b) AM-PM plots before applying the proposed DPD. Both, especially AM-PM plot, are relatively linear without DPD while the memory effect exists. Using the memory DPD, the signal fidelity is improved, which results in the low correlation loss at the receiver. The phase variation over instantaneous output power is flat. The random phase variation (3σ) is <±5.4 degrees and the corresponding group delay variation is <±9 ps when the normalized instantaneous amplitude is >0.5.

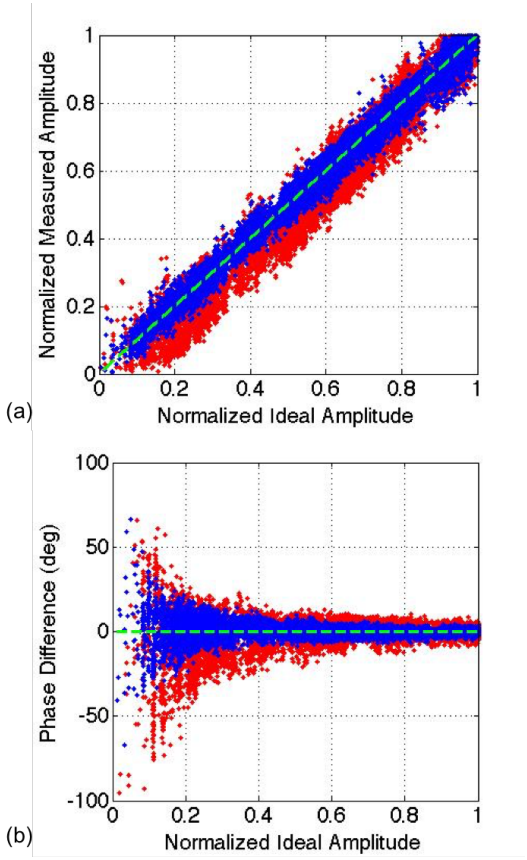

Fig. 9. Measured (a) AM-AM and (b) AM-PM plots before DPD (red dots) and after DPD (blue dots).

C. L2/L5-Band GaN SSPA Linearization

The effect of DPD is more significant for L2/L5 multi-carrier signal amplification. Fig. 10 shows the measured spectra of the L2/L5 composite signal before and after DPD when the signal is applied to a constant drain GaN SSPA. Before DPD, intermodulation products are emerged with the level of >-30 dBc due to the non-linearity of the SSPA. Using the MaXentric's DPD, the intermodulation products decreases to the level of the noise floor (<-50 dBc). The output power of the composite signal is 166 W_{arg}.

Fig. 10. Measured spectra of L2/L5 composite signal before and after DPD.

D. L1, L2 and L5-Band RF Front-End Sub-System

Fig. 11 shows the measured spectrum delivered from diplexer in the entire RF front-end sub-system prototype. A constant drain GaN SSPA is still used for the L2/L5 branch as a preliminary study. The total output power is 371 W_{arg}. Using the two-step DPD, the noise level due to the PA non-linearity is lower than -45 dBc.

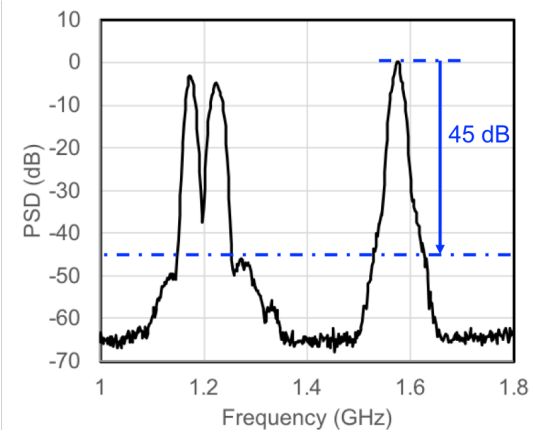

Fig. 11. Measured spectrum delivered from diplexer.

VI. Conclusion

A 370-W_{arg} high power RF front-end sub-system has been developed for GPS block-III satellite payload applications. Using the L1 and L2/L5 dual-path configuration instead of triple paths, the insertion loss of the multiplexer is improved from 0.2 dB to 0.8 dB. The developed GaN SSPA under envelope tracking operation amplifies the L1-band signal with the DE and PAE of 50% and 45% respectively. Using two-step DPD, the noise level due to the PA non-linearity is suppressed to lower than -45 dBc. The developed RF front-end sub-system gives future advanced global navigation satellite systems (GNSSs) more flexibility, such as output power control capability, increasing the number of codes and wider frequency operation.

Acknowledgment

This work was supported by Air Force Research Laboratory (AFRL) under Air Force SBIR program contracts (FA8650-11-C-7185. The authors would like to thank Dr. C. S. Mayberry, Dr. John S. Machuzak, Dr. Kenneth D. Bole, Dr. Kevin Slimak at AFRL, and Dr. James Staggs at ATA Aerospace for many valuable discussion and help. The authors also thank the teams at MaXentric, especially Dr. A. Mattson, C. Vu, D. Nguyen, B. Ghajari and J. Antonio for their contributions.

The views, opinions and/or findings expressed are those of the author and should not be interpreted as representing the official views or policies of the Department of Defense or the U.S. Government.

Appendix

The overall correlation loss is defined as the ratio of the useful power in the total transmitted power. The relationship between the overall correlation loss and NRMSE is expressed as

$$C.L. = -20\log_{10}\left(1 - \frac{NRMSE^2}{2}\right) \quad (2)$$

References

[1] J. W. Betz, "Something old, something new," *Inside GNSS*, pp. 34-42, July/Aug. 2013.

[2] R. Giofre, et. al., "A 300 W complete GaN solid state power amplifier for positioning system satellite payloads," in *Proc. IEEE Int. Microw. Symp.*, 2016, pp. 1-3.

[3] A. Katz, et. al., "High-efficiency high-power linearized L-band SSPA for navigational satellites," in *Proc. IEEE Int. Microw. Symp.*, 2017, pp. 1-4.

[4] J. J. Yan, et. al., "High-efficiency, high-linearity envelope tracking power amplifier for mobile UHF applications," in *Proc. MILCOM*, 2010, pp. 1572-1576.

[5] R. D. Harris, "Radiation Characterization of commercial GaN devices," in Proc. *IEEE REDW*, 2011, pp. 1-5.

[6] J. J. Yan, T. Nakatani, P. Theilmann, and D, F. Kimball, "A 500 MHz Portable Evaluation Platform for Digital Pre-Distortion and Envelope Tracking Power Amplifiers," *Proc. IEEE ARFTG,* May 2015.

[7] D. Wolk, et. al., "An investigation of the effect of fringing fields on multipactor breakdown," in *Proc. ESA-ESTEC MULCOPIM*, 2005, pp. 93-99.

[8] J. Kim, K. Konstantinou, "Digital predistortion of wideband signals based on power amplifier model with memory," *IET Electron. Lett.*, vol. 37, no. 23, pp. 1417-1418, Aug. 2002.

[9] IS-GPS-200H, [Online] https://www.gps.gov/technical/icwg/IRN-IS-200H-001+002+003_rollup.pdf.

[10] IS-GPS-800D, [Online] https://www.gps.gov/technical/icwg/IS-GPS-800D.pdf.